Excitation functions of pion reactions on ^{14}N, ^{16}O, and ^{19}F through the (3,3) resonance*

Norman P. Jacob, Jr.,† and Samuel S. Markowitz
Lawrence Berkeley Laboratory and Department of Chemistry, University of California, Berkeley, California 94720
(Received 8 September 1975)

Cross sections for pion-induced reactions of the form $(\pi, \pi N)$ and more complex spallation reactions of the form (π, X) have been measured from 50–550 MeV on the target nuclei ^{14}N, ^{16}O, and ^{19}F using the secondary pion beams at the Lawrence Berkeley Laboratory 184-inch synchrocyclotron and the Clinton P. Anderson Meson Physics Facility. The dominance of the (3, 3) free-particle resonance is seen in all excitation functions determined in this work. Relative to the $^{12}C(\pi^{\pm}, \pi N)^{11}C$ reactions, the $(\pi^{\pm}, \pi N)$ reactions on ^{14}N, ^{16}O, and ^{19}F have magnitudes of 0.2, 1, and 0.7, respectively. The cross section ratio $R = \sigma(\pi^-, \pi^- n)/\sigma(\pi^+, \pi N) = 1.68 \pm 0.18$ for ^{14}N at 188 ± 15 MeV, 1.68 ± 0.05 for ^{16}O at 188 ± 9 MeV, and 1.68 ± 0.03 for ^{19}F at 178 ± 2 MeV incident pion energy. The results from this work are compared to previous pion work, analogous proton-induced reactions, Monte Carlo intranuclear cascade-evaporation calculations, and to a semiclassical nucleon charge-exchange model which convincingly explains the $(\pi, \pi N)$ reaction mechanism in the (3, 3) resonance region.

[NUCLEAR REACTIONS $^{14}N(\pi^{\pm}, \pi N)^{13}N$, $^{16}O(\pi^{\pm}, \pi N)^{15}O$, $^{19}F(\pi^{\pm}, \pi N)^{18}F$, $^{14}N(\pi^{\pm}, X)^{11}C$, $^{16}O(\pi^{\pm}, X)^{13}N$, ^{11}C, and $^{19}F(\pi^{\pm}, X)^{11}C$, $E = 50$–550 MeV. Measured and calculated $\sigma(E)$, comparison to nucleon charge-exchange model.]

I. INTRODUCTION

"Simple" pion-induced reactions of the form $(\pi, \pi N)$, where N is the removed nucleon, have been the topic of numerous experimental investigations related to free-particle πN collisions in the nucleus.[1-18] Two major studies have generated considerable interest in this area. The first was the work of Reeder and Markowitz,[1] which showed a broad peak at 180 MeV in the $^{12}C(\pi^-, \pi^- n)^{11}C$ excitation function. This particular observation was not only ascribed to the dominance of the (3, 3) free-particle resonance, but was also interpreted in terms of a clean-knockout (CKO) mechanism. Later, the survey by Chivers *et al.*[8] of pion reactions on light nuclei using both $\pi^{\pm}$ and π^- presented the surprising result that the ratio of cross sections $R = \sigma(\pi^-, \pi^- n)/\sigma(\pi^+, \pi N)$ for ^{12}C, ^{14}N, and ^{16}O was 1.0 ± 0.1 at 180 MeV, in contrast to a simple impulse approximation or free-particle ratio of $R = 3$. Other determinations of $(\pi, \pi N)$ ratios at various pion energies for ^4He through ^{64}Zn have also shown disagreement with simple impulse approximation ratios.[9-17] Most noteworthy of these recent measurements is the redetermination of the $^{12}C(\pi^{\pm}, \pi N)^{11}C$ excitation functions by Dropesky *et al.*[18] which indicates a value of $R = 1.55 \pm 0.10$ at 180 MeV.

The above mentioned works have also served to stimulate theoretical interest in this area. Originally, these theories[19-21] were focused on reproducing the shape and magnitude of the $^{12}C(\pi^-, \pi^- n)$-^{11}C excitation function. Following the Chivers *et al.*[8] results, a number of theories[22-28] were proposed to explain the observed deviation from the impulse approximation model. Of these proposals, the semiclassical nucleon charge-exchange (NCE) model of Sternheim and Silbar[28] as applied to the $^{12}C(\pi^{\pm}, \pi N)^{11}C$ data of Dropesky *et al.*,[18] has provided the most convincing interpretation of the $(\pi, \pi N)$ reaction mechanism to date.

The general aim of this study was to probe the relationship of free-particle interactions to pion-nucleon interactions in the nucleus. The method employed was radioactivation mainly using the high intensity pion beams at the Clinton P. Anderson Meson Physics Facility (LAMPF). The target nuclei ^{14}N, ^{16}O, and ^{19}F are particularly amenable to this work because their constituent nucleons are essentially all on the "surface" where knockout reactions are thought to occur. In addition, the product radiations were readily detected.

II. EXPERIMENTAL PROCEDURE

Irradiations for this study were initiated using the secondary pion beams of the Lawrence Berkeley Laboratory (LBL) 184-inch synchrocyclotron and completed using the more intense pion beams of LAMPF. General pion beam characteristics for the Meson and Physics Caves at LBL and the high energy pion (P^3) and low energy pion (LEP) channels at LAMPF are summarized in Table I. All results in this work were obtained by either

TABLE I. Pion beam characteristics.

Channel	Particle intensities [a] (for π^+ and π^-) (sec^{-1})	Momentum resolution $\Delta p/p$ FWHM (%)	Contamination [b] (%)
Meson Cave (LBL)	10^5	10	17 μ^-, e^- for 100 MeV π^-
Physics Cave (LBL)	10^5–10^6	5–8	7–8 $\mu^\pm, e^\pm$ for 260–300 MeV $\pi^\pm$
High energy pion (P^3)	10^5–10^7	2–10	60 μ^-, e^- for 100 MeV π^-
			30 μ^+, e^+ for 100 MeV π^+
			<10 $\mu^\pm, e^\pm$ above 350 MeV $\pi^\pm$
			<5 P above 350 MeV π^+
Low energy pion (LEP)	10^5–10^7	0.1–4	10 μ^+, e^+ for 100 MeV π^+
			25 μ^-, e^- for 100 MeV π^-
			<1 $\mu^\pm, e^\pm$ for 220 MeV $\pi^\pm$

[a] On target.
[b] Information acquired from groups responsible for beam lines.

interrupting physics experiments at LBL for short independent exposures, or in a parasitic or independent manner with the Nuclear Chemistry Group[18] at LAMPF.

The target stack used in each irradiation consisted of two machined disks of equal diameter and thickness, one being a disk of either plastic scintillator or polyethylene, and the other being a primary target disk of either boron nitride, Teflon, or a can of boric acid, serving as targets for ^{14}N, ^{19}F, and ^{16}O, respectively. A summary of target dimensions and chemical compositions is given in Table II. Generally, disks with dimensions 3.7 cm in diameter by 0.6 cm thick were used. The plastic disk was always the first target to receive the beam, and served as a beam intensity monitor using the $^{12}C(\pi^\pm, \pi N)^{11}C$ reaction, for which cross sections from 50–550-MeV incident pion energy are known.[29] Times of bombardment were 10–20 min for boron nitride targets, 10–40 min for Teflon targets, and 2–4 min for boric acid targets. Periodic exposure of dummy targets outside the pion beam revealed no significant contribution to the observed product nuclides from the stray neutron background in the secondary channels.

TABLE II. A summary of pion targets.

Target nucleus	Target material	Empirical formula	Diameter (cm)	Thickness (cm)	Surface density (g/cm^2)	Chemical composition
^{12}C (monitor)	Pilot B [a] plastic scintillator (polyvinyltoluene)	$CH_{1.1}$	3.8–5.0	0.3–1.3	0.3–1.3	91.4% C 8.5% H <0.2% impurities
	Polyethylene	$(CH_2)_n$	5.0–6.3	0.6–1.3	0.6–1.2	85.4% C 14.4% H <0.2% impurities
^{14}N	Boron nitride	BN	3.8–5.0	0.3–1.3	0.6–2.6	41.5% B [b] 53.7% N 1.5–2.5% O <1% B_2O_3
^{16}O	Boric acid (in 0.013 cm Al can)	H_3BO_3	5.0	1.3	1.1–1.4	77.6% O 17.4% B 4.9% H <0.1% sulfates, metals, phosphates
^{19}F	Teflon (polytetrafluoroethylene)	$(CF_2)_n$	3.8–5.0	0.3–1.3	0.6–2.6	75.8% F 24.0% C 0.2% impurities

[a] Obtained from Pilot Chemicals Division, New England Nuclear Corporation, Watertown, Massachusetts.
[b] D. Malone (private communication).

Two positron annihilation (511–511 keV) coincidence detectors, each composed of a pair of 7.5-cm × 7.5-cm NaI(Tl) crystals oriented at 180°, were used to count the target activity. Decay characteristics and half-lives of the observed nuclides are given in Table III.[30] The carbon monitor and primary target disks were wrapped in copper jackets (0.03, 0.05, 0.1, and 0.1 cm for the Teflon, plastic, boron nitride, and boric acid target, respectively) to ensure annihilation of all emitted positrons close to the source; they were then counted in identical geometries between the NaI(Tl) scintillators. Because the monitor and primary target dimensions were equal, the efficiency for detection of positron annihilation quanta would also be equal for each disk, aside from self-absorption corrections. Thus *relative* and ultimately *absolute* cross sections may be obtained without measurement of absolute detection efficiency. The background measured less than 2 counts/min for the detector used for the boron nitride and Teflon targets, and from 15–25 counts/min for the detector used exclusively for the boric acid target. Location of the oxygen target detector near the beam area is the cause of this high background.

A Teflon irradiation in which the beam was monitored directly by a counter telescope required measurement of the coincidence efficiency of one γ-γ detector. This was accomplished by determining the absolute decay rate of ^{11}C in an irradiated plastic scintillator disk of dimensions equal to the Teflon disk in a β-γ coincidence detector, and then by counting the positron annihilation γ rays with the γ-γ coincidence detector. Care was taken to ensure that the activated area in the plastic disk was very nearly equal to that produced by the beam spot in the actual exposure. A final γ-γ detector efficiency for a 3.7-cm-diam by 0.6-cm-thick disk of Teflon located approximately 1 cm from the face of each NaI(Tl) crystal was (9.5 ±0.5)%.

All decay curves were fitted by the standard least squares program CLSQ[31] using the fixed half-lives in Table III for each radioactive component.

For the ^{16}O target, 71-sec ^{14}O was formed in such relatively low yield that it could be ignored in the decay curve without significantly effecting the end-of-bombardment activities of the other components.

Where necessary, corrections were made to the data for beam fluctuations (< 5%), proton contamination in the high energy (>350 MeV) π^+ beams at LAMPF (< 5%), and self-absorption of detected 511-keV annihilation quanta (3–10%). Results from the exposure of two different total target thicknesses of 1.25 and 2.54 cm (plastic monitor plus primary target) at several different pion energies for both π^+ and π^- revealed no significant change in cross section outside of statistical errors to warrant correction. Corrections for muon and electron activation were ignored because of the weakly interacting nature of these leptons. Details of these considerations are given elsewhere.[32]

TABLE III. Decay characteristics for the observed radionuclides (Ref. 30).

Nucleus	Half-life (min)	Fraction of decays leading to β^+ emission
^{11}C	20.4	1.0
^{13}N	9.96	1.0
^{15}O	2.05	1.0
^{18}F	109.8	0.97

III. RESULTS

The cross sections for the $(\pi^\pm, \pi N)$ and other more complex spallation reactions are displayed in Figs. 1 and 2. A total of 66 irradiations were made during this study, with duplicate cross section measurements performed whenever possible, particularly in the (3, 3) resonance region. Overlap in energy of pion cross section measurements among the various LBL and LAMPF pion channels was excellent.

The effective bombarding energy was taken as the pion energy at the midpoint of the target stack. Corrections to the initial pion energies for energy losses in passing through upstream targets were made. The spread in a particular pion energy is the root-mean-square combination of the beam momentum resolution, and the energy loss of a pion in traveling from the face of the disk stack to its midpoint. The range-energy curves of Trower[33] were used for calculating these energy losses.

Errors on the reaction cross sections are purely statistical, and were established from the root-mean-square combinations of standard deviations of the end-of-bombardment activities for product nuclides in the monitor and primary target disks as given by CLSQ.[31] Generally, these errors were conservatively 10%, 5%, and 3% for the $(\pi, \pi N)$ cross sections for ^{14}N, ^{16}O, and ^{19}F, respectively, and about 10% or less for the more complex spallation reactions. Where duplicate measurements were made, a weighted mean and standard deviation were calculated.

The only dominant systematic error for the pion results may be attributed to the 5–10% accuracy of the $^{12}C(\pi^\pm, \pi N)^{11}C$ monitor cross sections.[18]

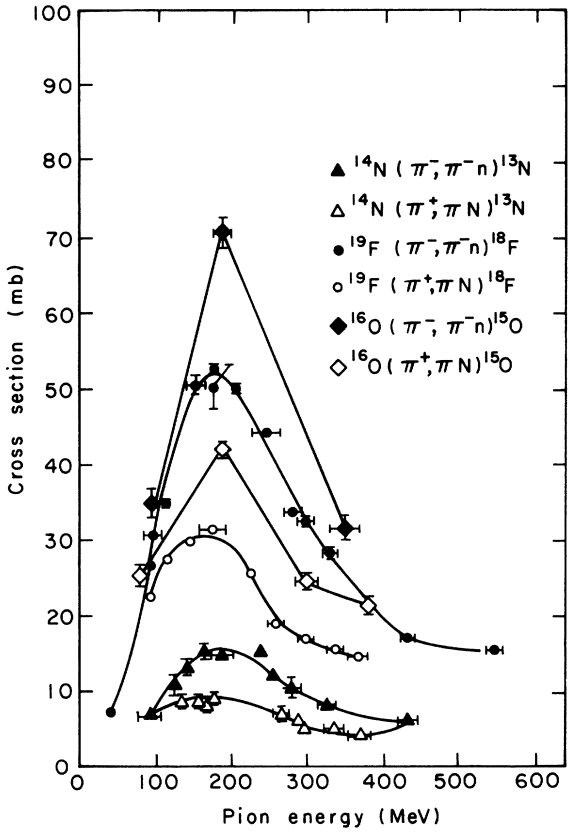

FIG. 1. (π, πN) excitation functions. Solid lines have been drawn through the experimental points as visual aids.

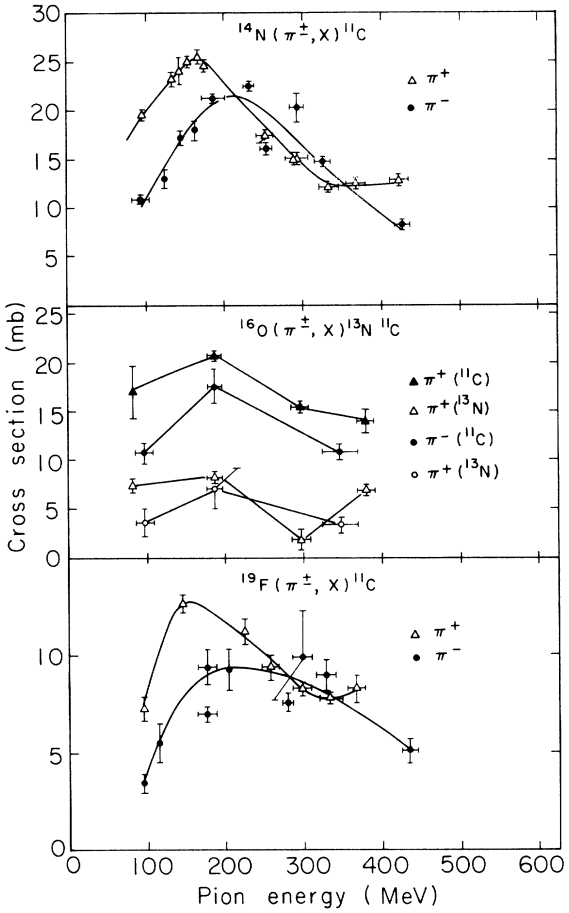

FIG. 2. Complex spallation excitation functions. Solid lines have been drawn through the experimental points as visual aids.

Thus, the total root-mean-square error in absolute cross section determination would vary from about 5–15%. The errors subsequently quoted for the ratio R do *not* include the 5–10% error in accuracy of the monitor cross sections. Errors for the ^{19}F($\pi^\pm$, X)^{11}C cross sections are large (~25%) due to large corrections applied to extract these cross sections from the gross $CF_2 + \pi \rightarrow {}^{11}$C reaction.

It should be pointed out that the ^{11}B(π^+, π^0)^{11}C reaction contributes to the plotted ^{14}N(π, X)^{11}C (target BN) and ^{16}O(π, X)^{11}C (target H_3BO_3) excitation functions. Based on a measured cross section for ^{11}B(π^+, π^0)^{11}C of 5 mb at 180 MeV from the work of Chivers *et al.*[8] it is estimated that no more than 8% of the cross section displayed for these more complex reactions comes from the charge-exchange reaction. No correction was applied for this effect.

IV. DISCUSSION

A. Features and qualitative interpretation of the results

Figures 1 and 2 demonstrate that the (3, 3) pion-nucleon resonance is preserved not only in "simple" reactions of the form (π, πN) but also in more complex spallation reactions of the form (π, X), where X represents a number of emitted nucleons. These observations lend credence to the concept of quasifree pion-nucleon collisions in both types of reactions.

Figure 1 also illustrates striking differences in cross section magnitudes among the (π, πN) reactions. This comparison may be made more meaningful by employing the following procedure: By scaling all the ($\pi^\pm$, πN) curves to match the ^{12}C-$\pi^\pm$, πN)^{11}C results of Dropesky *et al.*,[18] one obtains two sets of "universal" π^+ and π^- excitation functions, displayed in Fig. 3. It is seen that:

(1) The universal π^- curve shows that the (π^-,π^-n) excitation functions for ^{12}C, ^{14}N, ^{16}O, and ^{19}F have the same shape, width [250 ± 20 MeV full width at half maximum (FWHM)], and peak maximum at 180–190 MeV.

(2) The universal π^+ curve shows that the (π^+, πN)

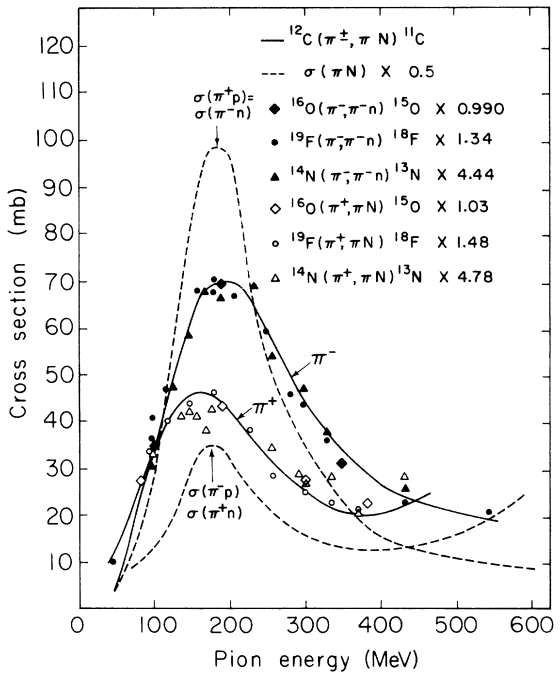

FIG. 3. Comparison of experimental excitation functions. The numbers given are factors by which an individual excitation function curve must be multiplied to fall on the "normal" $^{12}C(\pi,\pi N)^{11}C$ excitation function curve (Ref. 18). The free-particle cross sections, multiplied by a factor of 0.5, are also shown in the plot for comparison (Ref. 48).

excitation functions for ^{12}C, ^{14}N, ^{16}O, and ^{19}F have the same shape, width (also 250 ± 20 MeV FWHM), and peak maximum at about 180 MeV.

(3) The $(\pi,\pi N)$ excitation functions are considerably broader than the free-particle pion-nucleon resonances, which are about 140 ± 10 MeV FWHM.

(4) Cross sections for (π^-,π^-n) reactions on ^{14}N, ^{16}O, and ^{19}F relative to (π^-,π^-n) cross sections for ^{12}C are, respectively, 0.23 ± 0.02, 1.01 ± 0.06, and 0.75 ± 0.04 (indicated errors are standard deviations derived from individual relative cross sections).

(5) Cross sections for $(\pi^+,\pi N)$ reactions on ^{14}N, ^{16}O, and ^{19}F relative to $(\pi^{\pm},\pi N)$ cross sections for ^{12}C are, respectively, 0.21 ± 0.03, 0.97 ± 0.04, and 0.68 ± 0.03.

In emphasizing trends for the more complex reactions, we will refer only to the dominant reaction occurring in the target:

(1) The $^{14}N(\pi^+,X)^{11}C$ cross sections are somewhat larger than the $^{14}N(\pi^-,X)^{11}C$ cross sections below about 225 MeV, and at higher energies the excitation functions cross. At 350 MeV, the $^{14}N(\pi^+,X)^{11}C$ excitation function is seen to turn up relative to $^{14}N(\pi^-,X)^{11}C$.

(2) The $^{16}O(\pi^+,X)^{11}C$ cross sections are slightly larger than the $^{16}O(\pi^-,X)^{11}C$ cross sections, while the $^{16}O(\pi^{\pm},X)^{13}N$ excitation functions have equal magnitudes, within experimental error.

(3) The $^{19}F(\pi^+,X)^{11}C$ cross sections are larger than the $^{19}F(\pi^-,X)$ cross sections below about 250 MeV and are approximately equal until 325–350 MeV, where the π^+ curve begins to turn up relative to π^-. The errors on these complex ^{19}F cross sections are necessarily large, as mentioned previously, and thus, definitive comparisons should not be attempted.

(4) Some downshift in peak maximum to lower energies for the (π^+,X) excitation functions may be observed for ^{14}N and ^{19}F.

1. $(\pi,\pi N)$ cross section magnitudes

Insight into the difference in $(\pi,\pi N)$ cross section magnitudes seen in this study may be provided by a consideration of residual nucleus properties. A summary of the number of bound residual levels and the energy of the first excited unbound level for each residual product[34-36] is given in Table IV. The low $^{14}N(\pi,\pi N)^{13}N$ cross sections appear to be consistent with the proton instability

TABLE IV. Comparison of relative $(\pi,\pi N)$ cross section magnitude with residual nucleus stability.

Reaction	Number of bound residual levels	First particle unbound level (and emitted particle) (MeV)	Relative cross section
$^{12}C(\pi,\pi N)^{11}C$	10–12 [a]	8.4 (α) [a]	1
$^{14}N(\pi,\pi N)^{13}N$	1 [b]	2.4 (p) [b]	0.2
$^{16}O(\pi,\pi N)^{15}O$	7 [b]	7.6 (p) [b]	1
$^{19}F(\pi,\pi N)^{18}F$	≥20 [c]	5.4 (α) [c]	0.7

[a] Reference 34.
[b] Reference 35.
[c] Reference 36.

of all ^{13}N excited levels. In addition, it is seen that the relative cross section values may be qualitatively correlated to the magnitude of the first excited, particle unbound level. Further experimental examples would be required to either establish more firmly or refute this proposed explanation.

2. ($\pi, \pi N$) excitation function widths

As indicated in other work,[1,3,8,18] the broadening seen in ($\pi, \pi N$) excitation functions relative to the πN reaction is attributed to the Fermi motion of the struck nucleon. Qualitatively, the momentum distribution of the struck nucleon will cause a smearing out of the resonance because the center-of-mass energy has a range of values at each incident pion energy. In estimating then, the nucleon momentum effect, it would be necessary to average the πN cross section over the struck neutron momentum distribution, using for convenience, a Gaussian momentum distribution of the form $p^l e^{-p^2/p_0^2}$, where l is the angular momentum quantum number corresponding to the struck neutron shell, and p and p_0 are, respectively, the nucleon momentum and a parameter characteristic of this momentum.[37]

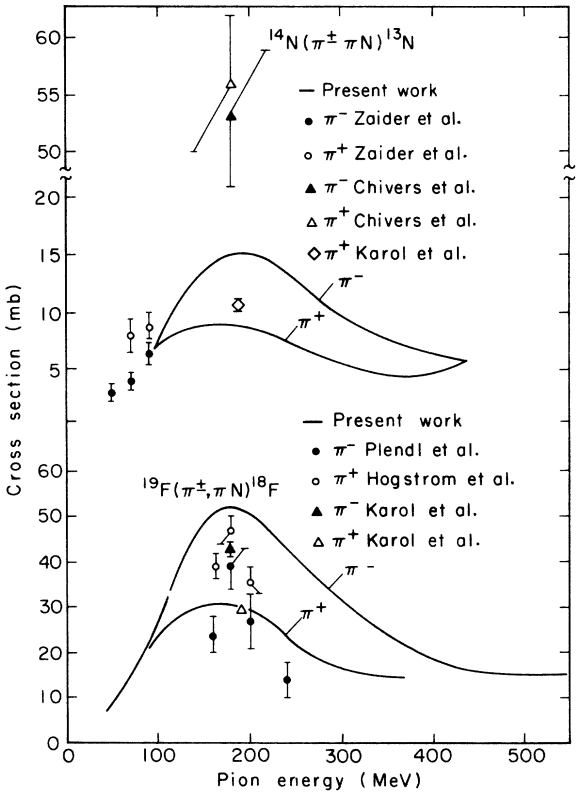

FIG. 4. Comparison of previous and present ($\pi^{\pm}, \pi N$) cross section measurements. References: Zaider *et al.* (Ref. 13), Chivers *et al.* (Ref. 8), Karol *et al.* (Ref. 16), Plendl *et al.* (Ref. 6), Hogstrom *et al.*(Ref. 7).

TABLE V. Comparison of π^-/π^+ cross section ratios for nucleon knockout near the (3, 3) resonance.

Reaction	Pion energy (MeV)	R_{π^-/π^+}	Reference
^{12}C($\pi, \pi N$)^{11}C	180	0.97 ± 0.09	8
	180	1.55 ± 0.10	18
^{14}N($\pi, \pi N$)^{13}N	180	0.95 ± 0.09	8
	188 ± 15	1.68 ± 0.18 [a]	present work
^{16}O($\pi, \pi N$)^{15}O	188	1.02 ± 0.09	8
	188 ± 9	1.68 ± 0.05	present work
	215	1.8 ± 0.4 [b]	14
	180	1.7 ± 0.4 [b]	15
^{19}F($\pi, \pi N$)^{18}F	190	1.52 ± 0.05	16
	178 ± 2	1.68 ± 0.03	present work
	184	1.11 ± 0.14 [c]	17

[a] The π^+ cross section used to calculate this ratio was interpolated from the excitation function.

[b] Ratio measured here is for $\pi^{\pm} + {}^{16}\mathrm{O} \rightarrow {}^{15}\mathrm{O}$, ^{15}N 6-MeV $\frac{3}{2}^-$ states.

[c] The cross sections used in this ratio were calculated relative to the ^{12}C($\pi, \pi N$) cross sections of Ref. 8.

Conversely, a quantitative estimate of the average momentum of the struck neutron may be obtained from a simpler approach. Using the formula derived by Reeder[38] and the value of 250 ± 20 MeV FWHM observed for the ($\pi, \pi N$) excitation functions in this work, and by using an average pion kinetic energy of 180 MeV, one obtains $p \approx 180$ MeV/c, a value consistent with the average momentum figures of $p \approx 160$–170 MeV/c for $1p$ protons in light nuclei.[37] Thus, the ($\pi, \pi N$) reaction may serve as a tool for measuring average "allowed" nucleon momentum.

3. Comparison to previous pion studies

Figure 4 illustrates comparison between prior and present ($\pi, \pi N$) cross sections for ^{14}N and ^{19}F. The ^{13}N cross sections appear to be in reasonably good agreement with the measured cross sections from the work of Zaider *et al.*[13] and Karol *et al.*,[16] but are in serious disagreement with the cross sections of Chivers *et al.*[8] at 180 MeV. As discussed previously, the low ^{13}N cross sections in this work are consistent with the instability of all excited ^{13}N levels. The ^{19}F($\pi^{\pm}, \pi N$)^{18}F excitation functions of Hogstrom *et al.*[7] and Plendl *et al.*[6] appear to be too narrow and do not exhibit the expected broadening of πN cross sections by the Fermi motion of the struck nucleon. Finally, the ^{16}O($\pi^{\pm}, \pi N$)^{15}O cross sections of Chivers *et al.*[8] at 180 MeV of 41 ± 4 mb for π^+ and 42 ± 4 mb for π^- are in good and poor agreement, respectively,

with the corresponding cross sections from this work at 188 MeV of 42 ± 4 mb and at 71 ± 7 mb, where the error includes that from the $^{12}C \rightarrow {}^{11}C$ monitor.

The ratio R, an important indicator of the $(\pi,\pi N)$ reaction mechanism, is compared for past and present work in Table V. For this study, $R = 1.68 \pm 0.18$ for ^{14}N at 188 ± 15 MeV, 1.68 ± 0.05 for ^{16}O at 188 ± 9 MeV, and 1.68 ± 0.03 for ^{19}F at 178 ± 2 MeV. The corresponding results are in poor agreement with the Chivers *et al.*[8] result of 1.0 ± 0.1, in fair agreement with the ^{18}F ratio of 1.52 ± 0.05 at 190 MeV from the work of Karol *et al.*,[16] and in good agreement with the ratios of 1.8 ± 0.4 and 1.7 ± 0.4 for $(\pi, \pi N)$ reactions on ^{16}O measured by Lieb *et al.*[14,15] These measurements, however, are still at variance with the impulse approximation value of 3 at 180 MeV. Close agreement is also observed between the ratios from this work and the value of $R = 1.55 \pm 0.10$ for the $^{12}C(\pi, \pi N)^{11}C$ reaction at 180 MeV.[18]

A broader comparison of the ratios from this work to those for the ^{12}C data as a function of incident pion energy is shown in Fig. 5. From this plot, it is seen that the values of R for $(\pi,\pi N)$ reactions on ^{12}C, ^{14}N, ^{16}O, and ^{19}F have similar energy dependences and nearly equal magnitudes. Such a comparison implies that the mechanism of

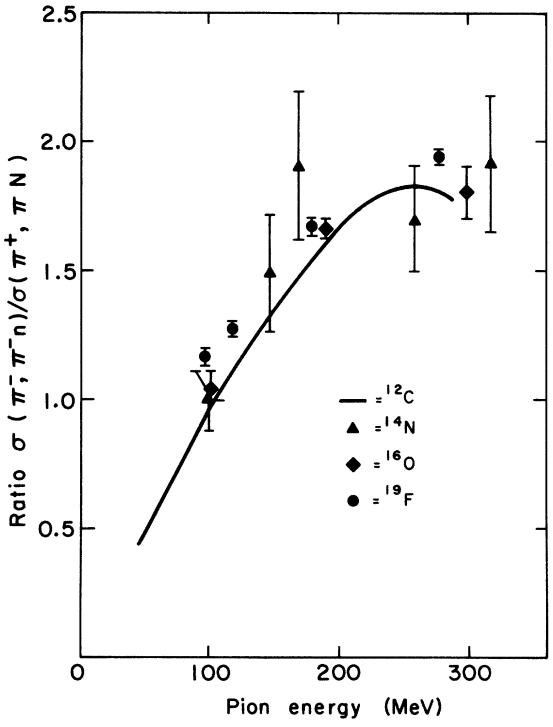

FIG. 5. Experimental $(\pi, \pi N)$ cross section ratios for ^{12}C, ^{14}N, ^{16}O, and ^{19}F. The ^{12}C ratios are from Ref. 18.

TABLE VI. Comparison between $(\pi, \pi N)$ and (p, pn) cross sections, relative to the $^{12}C \rightarrow {}^{11}C$ reactions.

Reaction	Relative cross section $\sigma(\pi^-\pi^-n)$	$\sigma(\pi^+\pi N)$	$\sigma(p,pn)$ [a]
$^{12}C \rightarrow {}^{11}C$	1.0	1.0	1.0
$^{14}N \rightarrow {}^{13}N$	0.23 ± 0.02	0.21 ± 0.03	0.16 ± 0.03 [b]
$^{16}O \rightarrow {}^{15}O$	1.01 ± 0.06	0.97 ± 0.04	1.31 ± 0.38 [c]
$^{19}F \rightarrow {}^{18}F$	0.75 ± 0.04	0.68 ± 0.03	0.65 ± 0.08 [d]

[a] Cross sections obtained from Ref. 40.
[b] Derived from cross sections in Ref. 40 above 200 MeV.
[c] Derived from cross sections in Ref. 40 above 400 MeV.
[d] Derived from cross sections in Ref. 40 above 460 MeV.

$(\pi, \pi N)$ reactions on these nuclei should also be similar.

Thus far, prior excitation function studies for pion-induced spallation of light targets in the (3,3) resonance energy region do not exist in the literature. The low energy 65 MeV $\pi^\pm$ spallation study on Cu^{39} has shown, as found in this work below 180 MeV, that π^+ cross sections are generally larger than those for π^-. Further work in complex pion-induced spallation reactions should become even more feasible with pion beams in excess of 10^8/sec at the various meson factories.

4. *Comparison to proton-induced reactions*

Since (a, aN) reactions at high incident projectile energies are expected to occur by similar mechanisms, it would be interesting to compare cross sections for (p,pn) reactions[40] to those for $(\pi,\pi N)$ reactions. Such a comparison would be especially valid for π^+ which like the proton, is a positively charged projectile.

This comparison of cross section magnitudes is summarized in Table VI. In synthesizing this summary, two approaches were used. First, all cross sections were determined *relative* to the $^{12}C \rightarrow {}^{11}C$ reaction for convenience of comparison. Second, since high energy (p,pn) excitation functions have similar shapes, as do the $(\pi, \pi N)$ reactions, it was possible to find only one "scaling" factor for each (p,pn) target. This method is entirely analogous to the normalization performed earlier for the comparison of $(\pi, \pi N)$ excitation function shapes. Such an approach is attractive because it allows a comparison of cross section magnitudes to be made over a broad energy range.

From Table VI, similarities between relative (p,pn) and $(\pi, \pi N)$ cross section magnitudes are seen. From this analysis, it appears that (1) the observed low cross sections for the ^{14}N-

TABLE VII. A comparison between cross sections for complex and proton reactions on light elements.

Reaction	Cross sections (mb) 260 MeV π^+ [a]	260 MeV π^- [a]	400 MeV p
$^{14}N \rightarrow {}^{11}C$	17.8 ± 1.8	19.5 ± 2.0	19.8 ± 2.0 [b,c]
$^{16}O \rightarrow {}^{11}C$	17.2 ± 1.8	14.4 ± 1.4	8.4 ± 0.8 [c]
$^{16}O \rightarrow {}^{13}N$	4.2 ± 1.0	5.5 ± 1.4	6.5 ± 0.7 [c]
$^{19}F \rightarrow {}^{11}C$	9.8 ± 2.5	8.4 ± 2.1	11.0 ± 2.3 [b,c]

[a] The cross sections at this energy were interpolated from the appropriate excitation function and assigned errors consistent with those observed experimentally.

[b] Reference 42; cross section adjusted to $\sigma_{^{27}Al}(^{24}Na) = 10.5$ mb.

[c] Reference 43; cross section adjusted to $\sigma_{^{12}C}(^{11}C) = 32.3$ mb.

$(\pi^{\pm}, \pi N)^{13}N$ reactions are consistent with low ^{14}N-$(p,pn)^{13}N$ results. (2) The (p,pn) and $(\pi, \pi N)$ reactions may proceed by similar mechanisms.

A comparison between high energy (p,X) and (π,X) reactions is somewhat more difficult than that made for $(\pi^{\pm}, \pi N)$ and (p,pn) reactions for several reasons. First, the (π,X) cross sections do not normalize to the $^{12}C(\pi, \pi N)^{11}C$ reaction as did the $(\pi, \pi N)$ reactions in this work. Furthermore, the cross section data for high energy (p,X) reactions on light nuclei in the lower GeV energy region (< 0.6 GeV) are scarce.

Still a limited but interesting comparison was made. Experimental[39] and theoretical[41] (Monte Carlo) studies have suggested that the yield distribution from pion-induced reactions should be about equal to those for protons with kinetic energies equal to the total pion energy. Thus Table VII gives a comparison of cross sections between 260 MeV pions and 400 MeV protons[42,43] on ^{14}N, ^{16}O, and ^{19}F. The similarities in cross section magnitudes between pions and protons tends to support the plausibility of this comparative approach. Comparisons at higher and lower energies could not be made due to a lack of pion and/or proton cross section data at the desired energies.

B. Mechanism of the $(\pi, \pi N)$ reaction

1. Monte Carlo calculations

The most recent high energy version of the VEGAS intranuclear cascade code[44] coupled to the DFF evaporation program[45] was used in this study to correlate the magnitude and general shape of the $(\pi, \pi N)$ [and (π,X)] excitation functions to a particular reaction model (cascade, including isobar formation and interaction, followed by evaporation) and nuclear model (Fermi gas, with a step distribution of nucleon density). Details concerning these programs are given elsewhere.[44,45]

Briefly, 5000 incident cascades with a pion potential of $V_{\pi} = 0$ were run for each target and projectile at 3 different energies, yielding a total of 18 theoretical $(\pi, \pi N)$ and 24 theoretical (π, X) cross sections. The energies chosen were about 100, 190, and 400 MeV in order to obtain an idea of the predicted energy dependence of the cross sections through the resonance energy. In addition to the absolute $(\pi, \pi N)$ cross section calculations, a supplemental subroutine was included with each program to determine the knockout $(\pi, \pi N)$ cross section. In these particular calculations, a knockout event was defined as one that produced a residual $(\pi, \pi N)$ cascade nucleus with less than the excitation energy needed to evaporate the least bound particle.

The DFF code[45] was first run to obtain these maximum excitation energies which were 10 MeV for ^{13}N (obviously too high), 9 MeV for ^{15}O, and 8 MeV for ^{18}F. The subroutine would then count knockout events in the list of cascade nuclei, and eventually calculate a knockout $(\pi, \pi N)$ cross section. It was hoped that such information would be useful in the interpretation of the $(\pi, \pi N)$ reaction mechanism.

One further adaptation was made. In the case of the $^{14}N(\pi, \pi N)^{13}N$ reaction, the knockout subroutine was used to choose only those residual ^{13}N nuclei with excitation energy less than 2.37 MeV, the energy of the first unbound level.

The computed $(\pi, \pi N)$ cross sections are presented first in comparison to the data in Figs. 6 through 8. Also shown are the calculations of Bertini,[46] which differ from the present code by

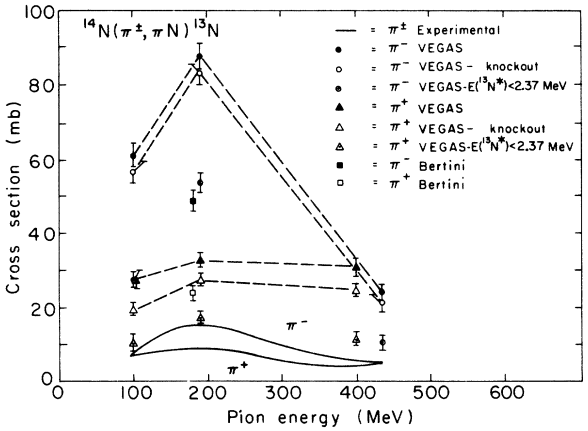

FIG. 6. Calculated and experimental $^{14}N(\pi^{\pm}, \pi N)^{13}N$ cross sections. The knockout cross sections were calculated assuming that the residual ^{13}N nucleus had less than 10 MeV of excitation energy. The case for which ^{13}N has less than the energy of its first (particle unbound) excited level is also shown. The results of Bertini (Ref. 46) are also displayed.

assuming that isobars formed within the nucleus immediately decay and thus do not interact as an integral unit.

The calculations show that $V_\tau = 0$ is satisfactory in reproducing the energy at which the peak maximum occurs and that the general energy dependence of the $(\pi, \pi N)$ reactions is correctly predicted. Fair agreement between the calculated and experimental cross sections is seen for the $^{16}O(\pi^\pm, \pi N)^{15}O$ reactions. The calculated ^{19}F-$(\pi^-, \pi^- n)^{18}F$ cross sections, however, are high by a factor of about 2, whereas the computed ^{19}F-$(\pi^+, \pi N)^{18}F$ cross sections are seen to be in good agreement with experiment. In addition, the calculation overestimates the ^{13}N cross sections, even when the particle instability of excited levels is taken into account.

The knockout cross sections, also plotted, are generally a high fraction of the total $(\pi, \pi N)$ cross sections; greater than 90% for $(\pi^-, \pi^- n)$ reactions and greater than 80% for $(\pi^+, \pi N)$ reactions on the light elements. Thus, these figures imply at most, that about 20% of the total $(\pi, \pi N)$ cross section may be ascribed to a pion inelastic (ISE) or charge-exchange (CESE, in the case of π^+) scattering followed by neutron evaporation. These percentages are consistent with the estimate of 85% for a CKO mechanism, deduced from an angular distribution study of the $^{12}C(p, pn)^{11}C$ reaction at 450 MeV,[47] and imply that some form of low energy deposition process may dominate the reaction mechanism.

A comparison among calculated, measured, and simple impulse approximation ratios[48] is given in Table VIII. The two most obvious trends are that:

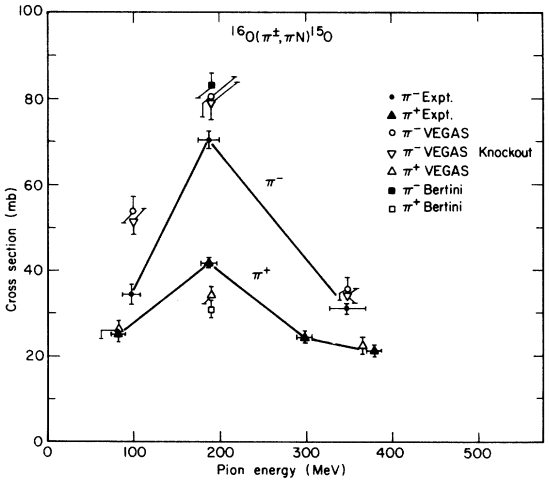

FIG. 7. Calculated and experimental $^{16}O(\pi^\pm, \pi N)^{15}O$ cross sections. The knockout cross sections were calculated assuming that the residual ^{15}O nucleus had less than 9 MeV of excitation energy. The results of Bertini (Ref. 46) are also given.

(1) The Monte Carlo results are always consistent with the simple impulse approximation or free particle ratios over the entire energy regime. (2) The Monte Carlo and simple impulse approximation or free-particle ratios are in disagreement with the experimental cross section ratios at the lowest two energies, but in excellent agreement at the highest energies (about 400 MeV) with the experiment. This last comparison implies that the CKO process dominates the $(\pi, \pi N)$ mechanism at pion energies exceeding about 350 MeV, but that the mechanism in the vicinity of the (3, 3) resonance is not as clearly understood.

Lastly, Table IX summarizes the cascade code estimates of isobar contribution to the $(\pi, \pi N)$ reaction. A requisite in compiling this table was that a $(\pi^\pm, I^\pm)$ event, where I is a pion-nucleon isobar, leave the residual nucleus with less excitation energy than necessary to evaporate the least bound particle (given by the DFF program). According to the calculation, the isobar process constitutes between 5–10% of the $(\pi, \pi N)$ cross section at the (3, 3) resonance energy of 180–190 MeV, and less than 2% at 100 and 400 MeV.

2. *Nucleon charge exchange (NCE)*

The concept of charge exchange of the outgoing nucleon in $(\pi, \pi N)$ reactions was initially considered by Hewson[27] relative to the data of Chivers *et al.*[8] This original theory, although it did not reproduce the result $R = 1.0 \pm 0.1$, did yield a π^-/π^+ cross section ratio that was between 1.6–1.9 at 180 MeV, in agreement with present experimental work.

The semiclassical NCE model of Sternheim and

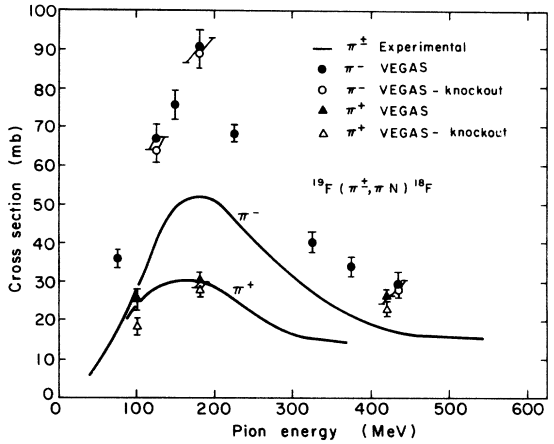

FIG. 8. Calculated and experimental $^{19}F(\pi^\pm, \pi N)^{18}F$ cross sections. The knockout cross sections were calculated assuming that the residual ^{18}F nucleus had less than 8 MeV of excitation energy.

TABLE VIII. Comparison of measured and calculated cross section ratios.

Nucleus	Pion energy (MeV)	Measured	Calculated VEGAS-DFF	Calculated Bertini [b]	Free particle [a] (impulse approx.)
^{14}N	100	0.99 ± 0.12 [c]	2.21 ± 0.20		2.50 ± 0.08
	190	1.68 ± 0.18	2.74 ± 0.23	2.04 ± 0.21	2.85 ± 0.10
	~418 [d]	0.98 ± 0.17 [e]	0.77 ± 0.08		0.83 ± 0.12
^{16}O	100	1.10 ± 0.11 [f]	2.06 ± 0.20		2.50 ± 0.08
	190	1.68 ± 0.05	2.36 ± 0.20	2.68 ± 0.10	2.85 ± 0.10
	~360 [g]	1.53 ± 0.15 [h]	1.58 ± 0.18		1.67 ± 0.06
^{19}F	100	1.17 ± 0.03 [i]	2.60 ± 0.25		2.50 ± 0.08
	180	1.68 ± 0.03	2.95 ± 0.23		1.95 ± 0.10
	~428 [j]	1.11 ± 0.11 [k]	1.01 ± 0.11		1.00 ± 0.06

[a] Reference 48.
[b] Ratios as calculated at 180 MeV; Ref. 46.
[c] Cross section ratio at 97 ± 10 MeV.
[d] Average of energies 400 MeV for π^+ and 435 MeV for π^-.
[e] Interpolated from excitation function.
[f] Interpolated ratio assuming relative ^{16}O$\xrightarrow{\pi}{}^{15}$O cross section figures given previously; cross section ratio at 98 ± 10 MeV.
[g] Average of energies 370 MeV for π^+ and 350 MeV for π^-.
[h] See footnote f; cross section ratio at 360 MeV.
[i] Cross section ratio at 96 ± 3 MeV.
[j] Average of energies 420 MeV for π^+ and 435 MeV for π^-.
[k] Interpolated ratio, assuming relative ^{19}F$\xrightarrow{\pi}{}^{18}$F cross section figures given previously.

Silbar,[28] conceptually similar to that by Hewson, has shown excellent agreement with the energy variation of the ratio R for the ^{12}C$(\pi, \pi N)^{11}$C reaction.[18] Following Sternheim and Silbar notation, the ratio of $(\pi, \pi N)$ cross sections is given by

$$R = [N\sigma_{\pi^-n}(1-P) + ZP\sigma_{\pi^-p\to\pi^-p}]/[N\sigma_{\pi^+n}(1-P) + ZP\sigma_{\pi^+p}], \quad (1)$$

where $\sigma_{\pi^-n} = \sigma_{\pi^+p}$ and $\sigma_{\pi^-p} = \sigma_{\pi^+n}$ are the free-particle cross sections, N and Z are the number of target neutrons and protons, respectively, and P is the probability of a nucleon charge exchange. The expression $P \propto [1 - \exp(-A\rho\sigma_{ex}d)]$, where σ_{ex} is the cross section for nucleon charge exchange, d is the mean distance traveled by a nucleon in the nucleus, A is the target mass number, and ρ is the nucleon density. The charge-exchange cross section contains one parameter which is fitted to an experimental point, usually at or near 180 MeV.[28]

TABLE IX. Contributions to the $(\pi, \pi N)$ cross sections as calculated by the ISOBAR VEGAS code (Ref. 44).

Nucleus	Pion energy (MeV)	$\sigma(I^-)$ (mb)	% of total $\sigma(\pi^-, \pi^-n)$	$\sigma(I^+)$ (mb)	% of total $\sigma(\pi^+, \pi N)$
^{14}N	100	1.0 ± 0.4	1.6 ± 0.6	0.2 ± 0.2	0.6 ± 0.6
	190	8.4 ± 1.2	9.5 ± 1.4	3.0 ± 0.7	9.5 ± 2.3
	400(π^+) 435(π^-)	0	0	0	0
^{16}O	100	1.0 ± 0.4	1.9 ± 0.8	0.64 ± 0.37	1.9 ± 1.1
	190	7.4 ± 1.1	9.1 ± 1.4	2.4 ± 0.6	6.8 ± 1.8
	350(π^-) 370(π^+)	0.68 ± 0.34	1.9 ± 1.0	0.2 ± 0.2	0.7 ± 0.7
^{19}F	100	1.5 ± 0.5	2.4 ± 0.8	0.2 ± 0.2	0.7 ± 0.7
	180	7.9 ± 1.2	8.7 ± 1.4	1.6 ± 0.5	5.2 ± 1.7
	435(π^-) 420(π^+)	0	0	0.54 ± 0.31	1.7 ± 1.0

The results for the ratios R on the light nuclei ^{14}N, ^{16}O, and ^{19}F from the Sternheim and Silbar[28] NCE model are displayed in Fig. 9 in comparison to the ratio of free-particle cross sections (π^-/π^+) and to ratios derived from the previously calculated Monte Carlo cross sections. The Monte Carlo calculations of Bertini[46] are also shown. All of the NCE curves have been normalized to an experimental point near 180 MeV.

The excellent agreement of the NCE model with the present data, and with the ^{12}C results, supports pion scattering followed by nucleon charge exchange as the dominant mechanism for the $(\pi, \pi N)$ reaction in the vicinity of the (3, 3) resonance. This excellent agreement is suprising in view of the fact that the NCE model encompasses an approach that is very similar to the Monte Carlo intranuclear-cascade method, which as demonstrated in Fig. 9, is in poor agreement with experimental R ratios in the vicinity of the (3, 3) resonance.

Beyond 350-MeV incident pion energy, the charge-exchange cross sections approaches zero, and therefore, the charge-exchange probability, as seen from the expression for P, also approaches zero. The result is that the theoretical ratio of $(\pi, \pi N)$ cross sections becomes equal, for $N = Z$ nuclei, to the ratio of corresponding free-particle pion-nucleon cross sections [Eq. (1)]. This limit is consistent with the observed excellent agreement among measured, Monte Carlo, and simple impulse approximation ratios above 350 MeV (Table IX).

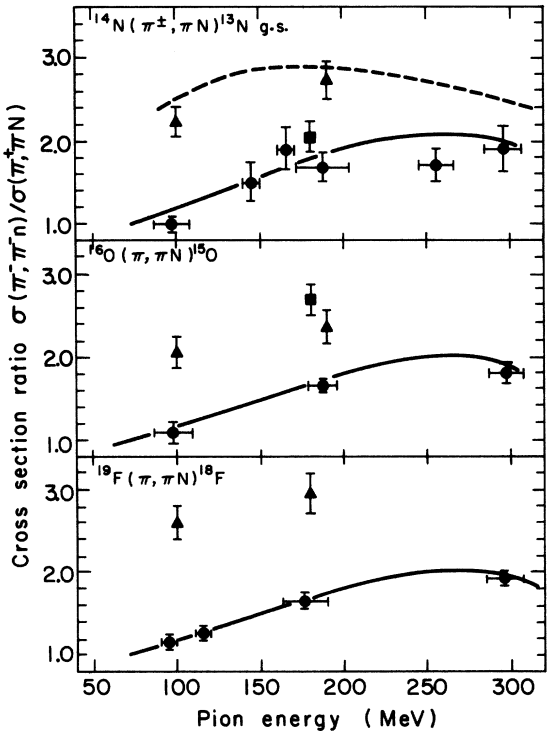

FIG. 9. Comparison of the NCE model to the measured ratios. The solid lines represent the theoretical NCE model, while the solid circles are experimental ratios. Other representations are: *dotted line*—free-particle πN ratios; *solid triangles*—the HEVI-DFF calculated ratios; *solid squares*—calculations by Bertini (Ref. 46).

C. Mechanism of (π, X) reactions

Several points may be established concerning more complex pion-induced spallation reactions from the limited results obtained in this work. Initial pion-nucleon collisions are important in these reactions, as seen by the dominance of the (3, 3) pion-nucleon resonance in the excitation functions for the (π, X) reactions. Noting that the inelastic (reaction) cross section for $\pi^- + {}^{12}$C exhibits a broad peak near 150 MeV,[49] one may also expect that the (π, X) reaction, which constitutes a fraction of the pion-nucleus reaction cross section, will display a similar energy dependence. Furthermore, the observed similarities in the yields of nuclei from protons and pions seen in the present and previous[39] work, indicate that the cascade-evaporation model, which has successfully correlated a large body of proton cross section data, is also applicable to the pion results. An important difference in the mechanism for energy transfer between protons and pions, however, is that a pion may either form a pion-nucleon isobar, which subsequently decays or interacts, or have its total energy absorbed between two nucleons. This absorption process has been suggested as the mechanism for pion interactions with nuclei between 0 and 60 MeV incident pion energy.[50] Even with increasing energy, its contribution to complex reaction mechanisms cannot be neglected. This is suggested by the excitation function for the $\pi^+ + d \rightarrow p + p$ reaction, which arises to a maximum in cross section of about 10 mb at 180 MeV and falls rapidly thereafter, where at 300 MeV it has a cross section of 2 mb.[51] Pion absorption in nuclear reactions has also been shown to be an important process in the VEGAS ISOBAR calculations of Harp *et al.*,[41] particularly for the production of nuclei far removed from the initial target.

A comparison of the measured (π, X) excitation functions to cross sections calculated at three pion energies by the previously mentioned cascade-evaporation code is displayed in Fig. 10. It may be seen that: (1) The influence of the (3, 3) resonance is correctly predicted in the excitation functions. (2) Agreement between experimental

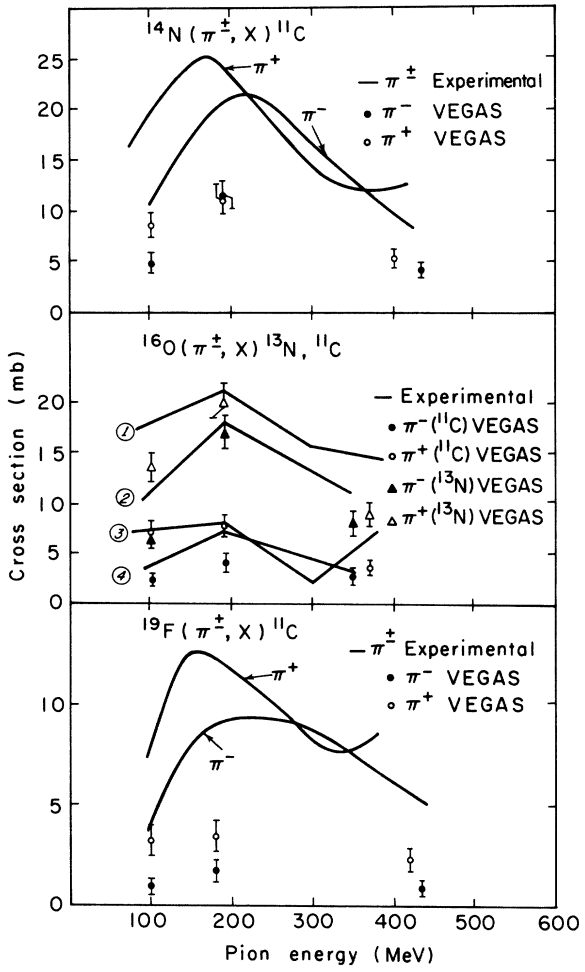

FIG. 10. Comparison of calculated and measured spallation cross sections. The middle diagram is labeled as follows: 1: $^{16}O(\pi^+,X)^{11}C$; 2: $^{16}O(\pi^-,X)^{11}C$; 3: $^{16}O(\pi^+,X)$-^{13}N; 4: $^{16}O(\pi^-,X)^{13}N$.

and calculated cross section magnitudes in all cases is poor. The cross sections for production of ^{11}C from ^{19}F and ^{14}N are much lower than the experimental values. The calculation overestimates again the ^{13}N cross sections. (3) Cross sections for π^+ for a given target and product are larger than the corresponding π^- cross sections at energies less than 180 MeV. At higher energies, the cross sections for the π^+ and π^- reactions become more equal. These calculated trends in (3) are generally consistent with those observed in the experimental excitation functions.

Thus, the Monte Carlo code appears to have reasonable success at predicting the energy dependence of pion-induced reactions, but generally gives poor agreement with experimental cross sections in this work.

V. SUMMARY AND CONCLUSIONS

The results of this study on pion-induced reactions may be briefly summarized. (1) The broad peaks that appear at about 180 MeV in the excitation functions for not only $(\pi^{\pm}, \pi N)$ but also for (π, X) reactions indicate the importance of initial pion-nucleon collisions in both types of reactions. (2) Striking differences in $(\pi, \pi N)$ cross section magnitudes may be related to the stability of the individual $(\pi, \pi N)$ product nuclei. (3) The measured ratio $R = \sigma(\pi^-, \pi^- n)/\sigma(\pi^+, \pi N) = 1.68 \pm 0.18$ for ^{14}N at 188 ± 15 MeV, 1.68 ± 0.05 for ^{16}O at 188 ± 9 MeV, and 1.68 ± 0.03 for ^{19}F at 178 ± 2 MeV. These values are consistent with the recently measured R value of 1.55 ± 0.10 for ^{12}C at 180 MeV. (4) Discrepancies between Monte Carlo and measured cross section magnitudes are perhaps due to the Fermi gas assumption incorporated into the cascade code, which for light nuclei is admittedly crude. In addition, the evaporation program assumes a continuum of excited states up to the first particle unbound level, which for the low Z residual nuclei in this work, is not applicable. (5) From the results in this study, the mechanism of the $(\pi, \pi N)$ reaction on light nuclei, a puzzle for some time, appears to consist of a mixture of knockout and nucleon charge exchange, with relatively small contributions from inelastic scattering followed by evaporation and isobar formation (2–10%) in the energy region from 100–350 MeV. Above 350 MeV, the clean knockout process dominates with small contributions possible from inelastic scattering followed by evaporation. With regard to pion charge exchange, recent work of Silbar[52] shows that for $^{12}C(\pi, \pi N)^{11}C$ from 50–300 MeV, the effect on R is negligible.

ACKNOWLEDGMENTS

We would like to thank the R. Haddock and K. Crowe groups at LBL and the Nuclear Chemistry group at LAMPF for allowing brief irradiations in their secondary pion beams, and for assistance in performing these irradiations. We are especially grateful to Dr. R. R. Silbar for performing and providing the NCE calculations and for informative discussions on this work; to Dr. G. Harp for discussions of the Monte Carlo results relevant to this study; to Dr. A. Poskanzer for helpful advice in the preparation of the original LAMPF proposal.

*Work supported by the U. S. Energy Research and Development Administration.

†Submitted in partial fulfillment of the Ph.D. requirements, Department of Chemistry, University of California, Berkeley. Present address: Nuclear Water and Waste Technology, San Jose, California.

[1]P. L. Reeder and S. S. Markowitz, Phys. Rev. 133, B639 (1964).

[2]A. M. Poskanzer and L. P. Remsberg, Phys. Rev. 134, B779 (1964).

[3]S. B. Kaufman and C. O. Hower, Phys. Rev. 154, 924 (1967).

[4]S. O. Thompson, L. Husain, and S. Katcoff, Phys. Rev. C 3, 1538 (1971).

[5]C. O. Hower and S. B. Kaufman, Phys. Rev. 144, 917 (1966).

[6]H. S. Plendl, D. Burch, K. A. Eberhard, M. Hamm, A. Richter, C. J. Umbarger, and W. P. Trower, Nucl. Phys. B44, 413 (1972).

[7]K. R. Hogstrom, B. W. Mayes, L. Y. Lee, J. C. Allred, C. Goodman, G. S. Mutchler, C. R. Fletcher, and G. C. Phillips, Nucl. Phys. A215, 598 (1973).

[8]D. T. Chivers, E. M. Rimmer, B. W. Allardyce, R. C. Witcomb, J. J. Domingo, and N. W. Tanner, Nucl. Phys. A126, 129 (1969).

[9]Y. A. Budagov, P. F. Ermolov, E. A. Kushinenko, and V. I. Muskalev, Zh. Eksp. Teor. Fiz. 42, 1191 (1961) [Sov. Phys.-JETP 15, 824 (1962)].

[10]M. A. Moinester, M. Zaider, J. Alster, D. Ashery, S. Cochavi, and A. I. Yavin, Phys. Rev. C 8, 2039 (1973).

[11]B. J. Lieb, H. O. Funsten, and W. K. Lankford, Bull. Am. Phys. Soc. 15, 596 (1970).

[12]M. V. Yester, A. A. Caretto, Jr., M. Kaplan, P. J. Karol, and R. L. Klobuchar, Phys. Lett. 45B, 327 (1973).

[13]M. Zaider, J. Alster, D. Ashery, S. Cochavi, M. A. Moinester, and A. I. Yavin, Phys. Rev. C 10, 938 (1974).

[14]B. J. Lieb, Ph.D. thesis, College of William and Mary, 1971 (unpublished).

[15]B. J. Lieb, H. S. Plendl, H. O. Funsten, W. J. Kossler, and C. E. Stronach, Phys. Rev. Lett. 34, 965 (1975).

[16]P. J. Karol, A. A. Caretto, Jr., R. L. Klobuchar, D. M. Montgomery, R. A. Williams, and M. V. Yester, Phys. Lett. 44B, 459 (1973).

[17]H. S. Plendl, D. Robson, C. J. Umbarger, D. F. Burch, and A. Richter, Bull. Am. Phys. Soc. 16, 1174 (1971).

[18]B. J. Dropesky, G. W. Butler, C. J. Orth, R. A. Williams, G. Friedlander, M. A. Yates, and S. B. Kaufman, Phys. Rev. Lett. 34, 821 (1975).

[19]V. M. Kolybasov, Yad. Fiz. 2, 144 (1965) [Sov. J. Nucl. Phys. 2, 101 (1966)].

[20]O. D. Dalkarov, Phys. Lett. 26B, 610 (1969).

[21]F. Selleri, Phys. Rev. 164, 1475 (1967).

[22]D. H. Wilkinson, J. Phys. Soc. Jpn. Suppl. 24, 469 (1968).

[23]R. Seki, Nuovo Cimento 9A, 235 (1972).

[24]V. M. Kolybasov, Phys. Lett. 27B, 3 (1968).

[25]V. M. Kolybasov and N. Ya. Smorodenskaya, Phys. Lett. 30B, 11 (1969).

[26]D. Robson, Ann. Phys. (N. Y.) 71, 277 (1972).

[27]P. W. Hewson, Nucl. Phys. A133, 659 (1969).

[28]M. M. Sternheim and R. R. Silbar, Phys. Rev. Lett. 34, 824 (1975).

[29]Taken from Ref. 18. The cross sections in this letter are subject to minor adjustment prior to final publication, R. A. Williams (private communication).

[30]C. M. Lederer, J. Hollander, and I. Perlman, *Table of the Isotopes* (Wiley, New York, 1966), 6th ed.

[31]J. B. Cumming, U. S. Atomic Energy Commission Report No. NAS-NS3107, 1962 (unpublished), p. 25.

[32]N. P. Jacob, Jr., Ph.D. thesis, Lawrence Berkeley Laboratory Report No. LBL-4067, 1975 (unpublished).

[33]W. P. Trower, University of California Lawrence Radiation Laboratory Report No. UCRL-2426, 1966 (unpublished), Vol. II.

[34]F. Ajzenberg-Selove, Nucl. Phys. A114, 1 (1968).

[35]F. Ajzenberg-Selove, Nucl. Phys. A152, 1 (1970).

[36]F. Ajzenberg-Selove, Nucl. Phys. A190, 1 (1972).

[37]M. Riou, Rev. Mod. Phys. 37, 375 (1965).

[38]P. L. Reeder, University of California, Lawrence Radiation Laboratory Report No. UCRL-10531, 1962 (unpublished).

[39]C. K. Garrett and A. L. Turkevich, Phys. Rev. C 8, 594 (1973).

[40]A. A. Caretto, Jr., U. S. Atomic Energy Commission Report No. NYO-10693, 1964 (unpublished).

[41]G. D. Harp, K. Chen, G. Friedlander, Z. Fraenkel, and J. M. Miller, Phys. Rev. C 8, 581 (1973).

[42]S. S. Markowitz, Ph.D. thesis, Princeton University, 1957 (unpublished).

[43]J. L. Symonds, J. Warren, and J. D. Young, Proc. Phys Soc. (Lond.) A70, 824 (1957).

[44]G. D. Harp, Phys. Rev. C 10, 2387 (1974).

[45]I. Dostrovsky, Z. Fraenkel, and G. Friedlander, Phys. Rev. 116, 1683 (1959).

[46]H. W. Bertini, Phys. Rev. C 6, 631 (1972).

[47]J. A. Panontin, L. L. Schwartz, A. F. Stehney, E. P. Steinberg, and L. Winsberg, Phys. Rev. 145, 754 (1966).

[48]E. Bracci, J. P. Droulez, E. Flamino, J. P. Hanson, and D. R. O. Morrison, CERN/HERA Report No. 72-1, 1972 (unpublished).

[49]F. Binon, P. Duteil, J. P. Garron, J. Barres, L. Hugon, J. P. Peigneux, C. Schmit, M. Spighel, and J. P. Stroot, Nucl. Phys. B17, 168 (1970).

[50]H. Ullrich, E. T. Boschitz, H. D. Engelhardt, and C. W. Lewis, Phys. Rev. Lett. 33, 433 (1974).

[51]Z. Fraenkel, Phys. Rev. 130, 247 (1963).

[52]R. R. Silbar, Phys. Rev. C 12, 341 (1975).